Turkish Journal of Immunology - Open Access
www.turkishimmunology.org

Turk J Immunol 2018; 6(3):108–117

Multi-Epitope Cluster Ep85B within the Mycobacterial Protein Ag85B Elicits Cell-Mediated and Humoral Responses in Mice

Ag85B Mikobakteri Proteini İçinde Yer Alan Çoklu Epitop Grubu Ep85B Farelerde Hücresel ve Sıvısal Yanıtı Düzenler

S.M. Touhidul ISLAM[1], Shabnam ZAMAN[1,2], Md Kawsar KHAN[1,2], Muhammad Ikhtear UDDIN[1], Sajib CHAKRABORTY[2], Naoshin Sharmin NISHAT[1], Nabilah IBNAT[1], Mohammad Murshid ALAM[1], Taufiqur Rahman BHUIYAN[1], Firdausi QADRI[1], Zeba I. SERAJ[2]

Abstract

Introduction: Epitope-based vaccines present a rational alternative to conventional concepts of vaccine design, particularly for combating complex infectious agents such as tuberculosis (TB). We have previously identified the multi-epitope cluster Ep85B, a linear 28 amino acid peptide within the mycobacterial Ag85B protein, which is capable of eliciting $CD4^+$ and memory $CD4^+CD45RO^+$ T-cell populations *in vitro* in human whole blood cells. In this report, we investigated the suitability of Ep85B for animal immunizations, and endeavored to demonstrate whether this epitope harbors the potential to induce both cell-mediated and humoral immune responses *in vivo*.

Materials and Methods: For immunization, BALB/c mice were injected subcutaneously with Ep85B. To test cellular immunity, splenocytes from the immunized mice were cultured in the presence of Ep85B and Th1/Th2 specific cytokine responses were analyzed by cytokine bead array. To test humoral immunity, Ep85B-specific IgG, IgM and IgA responses in serum collected from the immunized mice were determined by ELISA.

Results: Cytokine bead array displayed a significant increase of IFN-γ, IL-2 and TNF-α in the culture supernatant of splenocytes from the mice immunized with Ep85B compared to the naïve mice indicating the activation of a mixed Th1/Th2 cells. There was an increase of IgG and IgM antibody levels in the serum of mice immunized with Ep85B confirming the ability of the epitope to elicit humoral responses.

Conclusion: In silico predicted Ep85B epitope of mycobacterial Ag85B protein can elicit both cellular and humoral responses in mice.

Keywords: Immunoinformatics, epitope vaccine, tuberculosis, Ag85B

Öz

Giriş: Epitopa göre hazırlanmış aşılar, özellikle tüberküloz basili gibi karmaşık infeksiyon ajanlarına karşı geleneksel aşılardan farklıdır. Daha önce, mikobakterinin Ag85B proteini içinde yer alan 28 amino asitli lineer bir peptid olan çoklu epitop grubu Ep58B'nin, insan tam kan hücrelerinin kültüründe, *in vitro* olarak $CD4^+$ ve hafıza T hücre grubu olan $CD4^+CD45RO^+$ hücrelerini oluşturduğunu göstermiştik. Bu çalışmada, Balb/c fareleri, cilt altından uygulanan Ep85B ile bağışıklandı.

Gereç ve Yöntemler: BALB/c farelere Ep85B ile cilt altından bağışıklama yapıldı. Hücresel immün yanıtı incelemek için, bağışıklanmış farelerin dalakları Ep85B varlığında kültüre alındı ve Th1/th2 spesifik sitokin yanıtları sitokin boncuk yöntemi ile analiz edildi. Sıvısal bağışıklığı ölçmek için, bağışıklanmış farelerden alınan serumda Ep85B-ye özgün IgG, IgG, IgM ve IgA seviyeleri ELISA yöntemi ile ölçüldü.

Bulgular: Sitokin-boncuğu ölçümleri, Ep85B ile bağışıklanan farelerde IFN-γ, IL-2 ve TNF-α düzeylerinin, bağışıklanmamış fareler ile karşılaştırıldığında, karışık bir Th1/Th2 uyarımına işaret edecek ölçüde yükseldiğini gösterdi. Ayrıca, Ep85B ile bağışıklanmış farelerde IgG ve IgM düzeylerinin yükseldiği izlendi.

Sonuç: Mikobakterilerin Ag85B proteini içinde yer alan ve bilgisayar modelleme ile belirlenen Ep85B epitopu, farelerde hem hücresel hem de sıvısal bağışıklığı arttırır.

Anahtar Kelimeler: Bağışıklıkbilişimi, epitop aşısı, tüberküloz, Ag85B

[1] Centre for Vaccine Sciences, International Centre for Diarrhoeal Disease Research, Bangladesh (ICDDR,B), Dhaka, Bangladesh
[2] Department of Biochemistry and Molecular Biology, University of Dhaka, Bangladesh

Correspondence:
Zeba I. SERAJ
Department of Biochemistry and Molecular Biology, University of Dhaka, Bangladesh
E-mail: zebai@du.ac.bd

Received: May 12, 2018
Accepted: Sep 11, 2018

https://doi.org/10.25002/tji.2018.868

Introduction

Vaccines are traditionally composed of either selected immunogenic components of a pathogen, such as protein subunits, or the whole pathogenic cell itself in an inactivated or attenuated form. Although widely successful, this approach has proved overly simplistic

for combating infectious diseases that are more complex in nature, including tuberculosis (TB). Epitope-based vaccines provide a rational alternative to conventional design strategies, and progress in the field of immune-informatics has enabled the use of computational methods (*in silico*) to assess the immunogenic properties of proteins in a manner that is both systematic and highly effective.[1,2]

TB remains a leading cause of mortality from infectious disease throughout the world[3], and there were an estimated 8.6 million new TB cases and 1.3 million TB deaths in 2012 alone.[4] In spite of this situation of an impending epidemic, the only TB vaccine currently available is the live-attenuated *M. bovis*-derived Bacillus Calmette-Guerin (BCG), which offers incomplete, variable and often only transient protection against pulmonary TB, particularly in infants.[5–7] Although newly designed TB vaccine candidates are currently in different phases of development[8–11], these efforts have yet to replace or supplement the existing BCG, thereby further underscoring the need to establish novel methodologies for the design of TB vaccine candidates.

The identification of MHC ligands and T-cell epitopes is the most crucial aspect of TB vaccine design[12,13], given that protective immunity against *M. tuberculosis* is characterized by the ability to induce interferon-gamma (IFN-γ) and other type 1 T helper cell (Th1) cytokines by antigen-specific T cells.[14–18] For this purpose, a range of statistical and machine-learning algorithms have been specifically developed to assist in the *in silico* pre-screening of immunogenic epitopes. The identified peptides can then be synthesized in a chemically well-defined manner that is open to large-scale production, with the outcomes of several studies[19–21], including clinical trials[22–24], indicating the potential for similarly conceived peptide vaccination strategies.

We have previously identified a 28 amino acid multi-epitope cluster within the secretory protein Ag85B, a model mycobacterial antigen.[25] This region, termed Ep85B, has been shown to elicit significant increases in both $CD4^+$ and memory $CD4^+CD45RO^+$ T-cell populations when used to stimulate human whole blood cells *in vitro*. To determine the peptide's suitability for immunizations in animal models, we investigated the immune potential of epitopes contained in the Ep85B cluster. Based on our *in silico* results, the ability of Ep85B to elicit humoral and cell-mediated immune responses *in vivo* was experimentally validated using BALB/c mice.

Materials and Methods

Identification of murine T cell epitope clusters

Tools from the Immune Epitope Database (IEDB) (http://www.iedb.org) were utilized for the prediction of both helper T cell (Th) and cytotoxic T cell (CTL) specific epitopes within the conserved 310 amino acid sequence of Ag85B. A range of different algorithms were selected for peptide-MHC binding prediction: for Class I, Artificial Neural Network (ANN)[26], Average Relative Binding (ARB)[27] and Stabilized Matrix Method (SMM)[28] were used, whereas NN-align[29], SMM-align[30] and ARBpython[27] were employed for Class II. T cell epitopes were predicted on the basis of binding affinities between MHC molecules and putative epitope regions, each consisting of nine amino acids (9-mers). These binding affinities were represented by inversely proportional IC50 scores, and epitopes with scores lower than the cut-off threshold of 500 nm[26,31] were considered to be strong binders. For both Th and CTL epitopes, the IC50 value and count of unique alleles for each position were obtained from the data and analyzed. Indeed, MHC class-II restricted epitope consists of 13–15 amino acids. However, only 9 amino acids interact with the binding groove of the MHC molecule while the rest amino acids are flanking residues serving to appropriately position the peptide on MHC molecule.[32] Our predicted algorithms served to initially fragment the predicted peptide into 13–15-mer amino acids as well as a core 9-mer and to calculate the binding affinity of the core 9 mer vs. the 13–15 mer peptide. As only the 9-mers bind to the MHC groove, we used the 9-mer for further analysis.

Identification of B cell epitope clusters

To determine the presence of B cell epitopes within Ag85B, two techniques were applied: the Kolaskar Tangaonkar method[33] and the ABCpred algorithm[34], with accuracies of 75% and 68.93%, respectively. The Kolaskar and Tongaonkar algorithm identifies antigenic determinants of proteins by utilizing the physicochemical properties of amino acid residues, together with their frequencies of occurrence in experimentally validated segmental epitopes. In contrast, the ABCpred algorithm predicts B cell epitopes within a fixed window size using an artificial neural network approach.

Continuous B cell epitopes were predicted using both methods (with window size set to 16 for ABCpred), and amino acids with the highest position-specific antigenicity scores for both tools were chosen among all those available

for that position. For amino acids that are a constituent of multiple contiguous epitopes, we considered the overlapping position with the maximum antigenicity score. In order to identify B cell epitope dense regions, amino acid positions in Ag85B were divided as epitope dense, average and poor based on the antigenicity score by K-means clustering.[35] A heat map depicting amino acids with high, moderate and low antigenicity scores was generated and used to predict potential B cell epitope clusters.

Antigens and adjuvants

Ep85B and the conjugated Ep85B with keyhole limpet hemocyanin (Ep85B-KLH) were both synthesized commercially at 95% purity (1st Base, Singapore and CHI Scientific, MA, USA, respectively). The Ag85B purified antigen was provided by BEI Resources (VA, USA), and phytohemagglutinin (PHA) was obtained from Remel Inc. (Lenexa, KS, USA). Complete and incomplete Freund's adjuvants were obtained from Sigma, MO, USA.

Immunizations

The studies were performed using six-to eight-week old female BALB/c mice raised at the Animal Resource Branch (ARB) of the International Centre for Diarrhoeal Disease Research, Bangladesh (ICDDR,B). Approval for animal studies was procured from both the Research Review Committee (RRC) and the Animal Experiments Ethics Committee (AEEC) of ICDDR,B.

Two groups of mice (five in each group) were immunized with either Ep85B or Ep85B-KLH. The prime dose was administered with complete Freund's adjuvant via the subcutaneous route, whereas subsequent doses were provided with incomplete Freund's adjuvant and delivered via the intra-peritoneal route. For each dose, 50 μg of antigen was used with an equal volume of adjuvant, and immunizations were carried out at two-week intervals on days 0, 14, 28 and 42. Pre-immune blood was collected before immunization on day 0, followed by subsequent collections on days 14, 28 and 42, via tail bleed. On day 49, seven days after the last dose, blood was retrieved via heart puncture. The samples were allowed to clot at room temperature, after which they were centrifuged at 662 × *g* for 10 minutes. The resulting sera were removed and stored at-70°C.

Cytokine bead array (CBA)

Animals were euthanized on day 49, and splenocytes were processed from the spleens of naive mice as well as those immunized with either Ep85B or Ep85B-KLH. 5×10^5 splenocytes were cultured in RPMI 1640 (Gibco, USA) media supplemented with 10% FBS, 200 U penicillin, 200 μg streptomycin/mL, 2 mM L-glutamine and 50 μM β-mercaptoethanol for four days in the presence or absence of 1 mg/ml of Ep85B. On the fourth day, supernatants were analyzed to determine helper T cell subgroup dominance (Th1 or Th2) in the cultured splenocytes. This was indicated by the types of cytokine responses elicited upon antigen-specific stimulation using a five-bead (IL-2, IL-4, IL-5, IFN-γ and TNF-α) cytometric bead array kit (BD Biosciences, USA) and FACS caliber flow cytometry machine (BD Biosciences, USA). Representing the cytokine responses directly as concentration without normalization has the risk of introducing cell culture artifacts. Therefore, cytokine responses in the supernatants of the cultured splenocytes from naïve, Ep85B or Ep85B-KLH immunized mice were presented as stimulation index. Stimulation index was calculated by normalizing the concentration of a cytokine in the supernatant of the antigen-stimulated (Ep85B) splenocytes against the concentration of the same cytokine in the supernatant of the non-stimulated splenocytes.

Antibody responses

Ep85B-specific IgG, IgM and IgA responses were measured using an enzyme-linked immunosorbent assay (ELISA). Polystyrene plates featuring 96 wells (NUNC-F, Denmark) were coated with 1 μg/mL of Ep85B or Ep85B-KLH in phosphate-buffered saline (PBS). Following this, 100 μL sera from immunized mice (diluted 1:20 in 0.1% bovine serum albumin (BSA) (Sigma Aldrich) in PBS-0.05% Tween) was added to each well and incubated for 90 min at 37°C, after which the plates were washed thrice using PBS-0.05% Tween. Goat anti-mouse isotypes IgG, IgM or IgA (Southern Biotech, USA) antibodies conjugated to horseradish peroxidase (HRP) were then separately applied, and the plates incubated for 90 mins at 37°C followed by three consecutive washes with PBS-0.05%, and once with PBS for each plate. The plates were developed with ortho-phenyle diamine (Sigma, MO, USA) in 0.1 M sodium citrate buffer (pH 4.5) and 0.04% hydrogen peroxide, then read kinetically at 450 nm for 5 min. The maximal rate of change of optical density per minute was calculated in milli-absorbance units, and the data normalized using the ratio of the test sample values to those of the pooled sera prepared from terminal bleeds. To test the cross-reactivity of anti-Ep85B IgG in the sera with the whole Ag85B, Polystyrene plates featuring 96 wells were coated with 1 μg/mL of Ag85B or BSA in PBS. Following this, 100 μL sera from mice on day 0 or day 49 of immunization with Ep85B or Ep85B-KLH (diluted 1:20 in 0.1% BSA in PBS-0.05% Tween) were added to

each well and incubated for 90 min at 37°C. Then IgG specific ELISA was performed as described above.

Statistical analyses

Comparisons were made based on the magnitude of the elicited immune responses. When the data from independent groups of mice were compared, unpaired non-parametric t-test (Man-Whitney test) was used. When the data from different time points of the same group of mice were compared, unpaired parametric t-test was used. All reported P values are two-tailed, with a cut-off value of 0.05 considered to be a threshold for statistical significance. GraphPad Prism 7.0 was used for various analytical purposes.

Results

T and B cell epitope clusters in Ag85B

We identified murine T cell epitopes using IC50 values corresponding to the binding affinities between mouse MHC molecules and short 9-mer peptides. The immunogenic property of each epitope was characterized by its IC50 value, which indicates the peptide's binding capacity to MHC molecules and the number of corresponding restricting MHC alleles. The position distribution of IC50 values and the numbers of corresponding MHC alleles for each algorithm are visualized in Fig. 1. The entire length of the Ag85B protein is associated with a very low, almost uniform number of unique alleles, with the maximum count for each position not exceeding 2 in the analysis of Class II epitopes. This is likely due to the inclusion of only a limited number of mouse alleles in the IEDB database. As such, clustering analyses were not carried out for murine T cell epitopes.

Within the 150–177 aa epitope cluster region designated as Ep85B, the algorithms predicted a total of 7 and 8 epitopes that bind with mouse MHC Class I and MHC Class II molecules, respectively. Among these peptides, 6 MHC Class I and 2 MHC Class II binding peptides were predicted to bind with alleles specific to the BALB/c mouse haplotype (H-2-Dd, H-2-K^d, H-2-L^d, H-2-IA^d; Supplementary Tables 1 and 2), thus indicating the suitability of this strain for the evaluation of peptide immunogenicity.

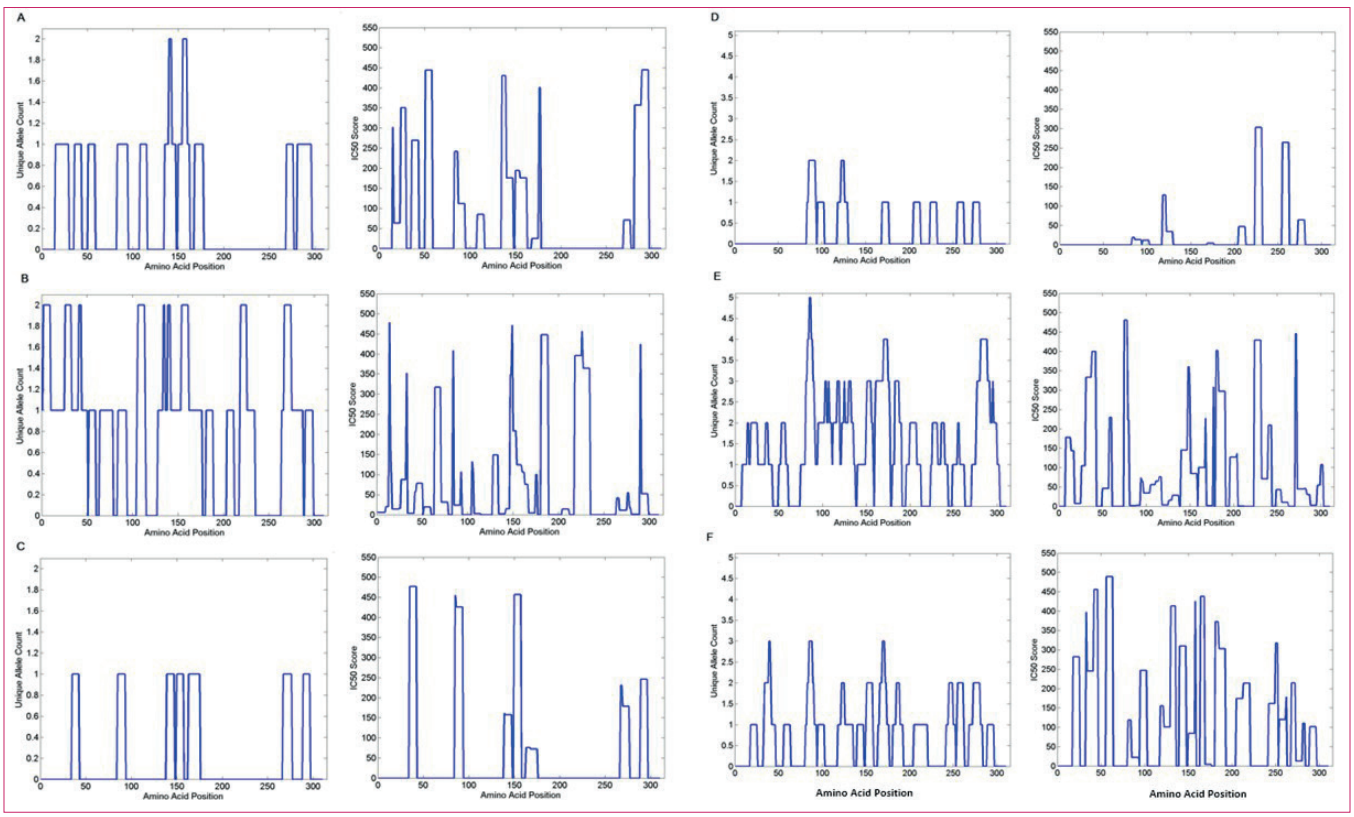

Figure 1. a–f. Unique allele counts and IC50 values at each amino acid position. For Th cell epitopes, the predictions were derived from the algorithms NN-align (a), ARBPython (b) and SMM-align (c). For CTL cell epitopes, the predictions were derived from the algorithms ANN (d), ARB (e) and SMM (f). The low IC50 values indicate the strong binding between epitope and MHC molecule whereas the higher unique allele counts specify the binding capability with higher MHC allele.

Turk J Immunol 2018; 6(3):108–117

Table 1. Th cell epitopes in Ep85B and their restricted murine MHC Class II molecules as predicted by the NN-align, ARBpython and SMM-align methods*

Epitope no.	Epitope sequence	Restricted MHCII
1	LSMAGSSAM [a]	H2-IAb
2	MAGSSAMIL [b]	H2-IAb
3	**GSSAMILAA** [c]	**H2-IAd,** H2-IAb
4	**SSAMILAAY** [b]	**H2-IAd**
5	LAAYHPQQF [c]	H2-IAb
6	YHPQQFIYA [d]	H2-IAb
7	QFIYAGSLS [c]	H2-IAb
8	FIYAGSLSA [e]	H2-IAb
9	IYAGSLSAL [c]	H2-IAb

* Peptides binding to BALB/c and their corresponding MHC Class II alleles (of the *d* haplotype) are shown in bold.
[a] Predicted by NN-align, ARBpython and SMM-align
[b] Predicted by NN-align
[c] Predicted by ARBpython
[d] Predicted by ARBpython and SMM-align
[e] Predicted by NN-align and SMM-align

Table 2. CTL cell epitopes in Ep85B and their restricted murine MHC Class I molecules as predicted by the ANN, ARB and SMM methods

Epitope no.	Epitope sequence	Restricted MHCII
1	**LSMAGSSAM** [a]	**H-2-Ld, H-2-Kd**
2	**SMAGSSAMI** [a]	**H-2-Kd**, H-2-Kk
3	**LAAYHPQQF** [b]	**H-2-Ld,** H-2-Kb
4	AAYHPQQFI [b]	H-2-Kb, H-2-Db
5	**HPQQFIYAG** [c]	**H-2-Ld**
6	QQFIYAGSL [c]	H-2-Kb
7	**IYAGSLSAL** [a]	**H-2-Kd**

Peptides binding to BALB/c and their corresponding MHC Class II alleles (of the *d* haplotype) are shown in bold.
[a] Predicted by ARB and SMM
[b] Predicted by ARB
[c] Predicted by SMM

The K-means clustering method has previously been used to differentiate between epitope dense and epitope poor segments[35], and was implemented in our study to identify regions with higher concentrations of epitopes. Accordingly, the algorithm revealed differential B cell epitope densities within the Ag85B antigen, as depicted in Fig. 2. The Kolaskar Tongaonkar algorithm predicted a linear B cell epitope ranging from 152–184 aa, whereas six epitopes identified by ABCpred overlapped with the region spanning Ep85B.

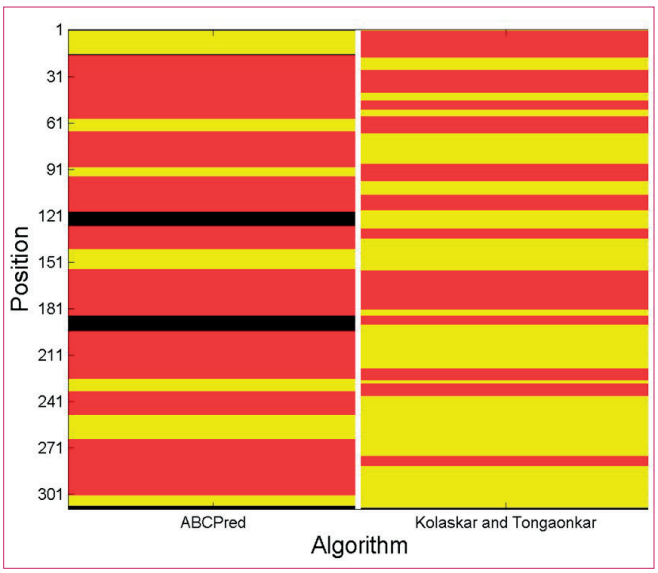

Figure 2. B-cell epitope clusters within Ag85B Epitopes were predicted using the Kolaskar Tangaonkar and ABCpred algorithms, and clusters were identified by the K-means method. Each amino acid is classified as high, medium or low on the basis of its antigenicity score. The color red denotes a high antigenicity score, yellow indicates a medium antigenicity score and black represents regions with no B-cell epitopes.

Immunization with Ep85B stimulates both Th1 and Th2 specific cytokine response

A cytometric bead array was performed to determine the Th subgroup dominance of Ep85B-induced culture supernatants of splenocytes from naive, Ep85B or Ep85B-KLH immunized mice. Both Th1 (IL-2, IFN-γ and TNF-α) and Th2 (IL-4 and IL-5) specific cytokine responses were detected in mice immunized with Ep85B and Ep85B-KLH, demonstrating the ability of Ep85B to stimulate cytotoxic immune responses (Fig. 3). For Th1 specific cytokine responses, IL-2 and TNF-α both exhibited minor but significant increases (~2-fold; $p<0.04$) in comparison with naïve controls. The most marked difference was observed for IFN-γ, where coupling of Ep85B with the carrier protein KLH resulted in 5-fold increases ($p=0.03$), while immunization with Ep85B alone elicited much lower responses (Stimulation Index of only ~1). Unlike other cytokines, significantly higher response of IFN-γ ($p=0.02$) was demonstrated in the case of immunization with Ep85B-KLH compared to the immunization with Ep85B alone. For Th2 responses, significant increases were detected for IL-4 ($p<0.04$), but no statistically significant difference was observed between the two forms of the peptide. This absence of significant differences between the conjugated and unconjugated variants of Ep85B, across all of the Th1 and Th2 specific cytokines studied, indicates that Ep85B is capable of stimulating a cytokine profile without the need for a carrier protein.

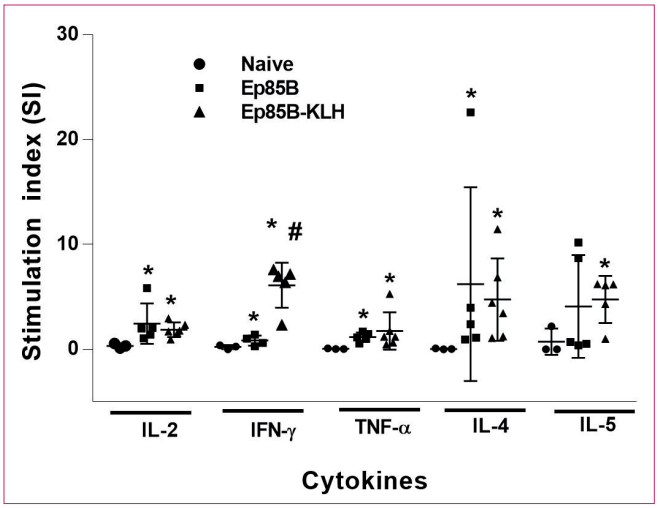

Figure 3. Th1 and Th2 specific cytokine responses in mice immunized with Ep85B or Ep85B-KLH. Splenocytes from naive, Ep85B or Ep85B-KLH immunized mice were cultured in the presence of Ep85B and analyzed for cytokine responses using a cytokine bead array. circular, square and triangular dark-filled dots represent the readouts for stimulation of splenocytes from naive, Ep85B or Ep85B-KLH immunized mice, respectively. An asterisk and hash sign denotes statistical significance ($p<0.05$) compared to the naïve and Ep85B cohorts respectively performed by unpaired non-parametric t-test (Man-Whitney test). the error bars represent standard errors of the mean. Data are shown from one immunization experiment, n=3–6.

Immunization with Ep85B elicits specific antibody responses

Ep85B-specific IgG, IgM and IgA antibody responses were measured in mice immunized with either Ep85B or Ep85B-KLH. Significantly higher levels of serum anti-Ep85B IgG responses were detected in both Ep85B and Ep85B-KLH immunized mice, and these remained elevated up to day 49. All cohorts of mice immunized with Ep85B and Ep85B-KLH were seroconverted (i.e., two-fold increase of antibody responses) after the third or fourth dose, with a mean fold increase of 4.4 and 3.6, respectively, when compared to their corresponding baselines. Similarly, significant increases in anti Ep85B-IgM antibody responses were detected after the third dose of immunizations in both Ep85B and Ep85B-KLH immunized mice, when compared to pre-immune sera (Fig. 4). Comparisons of Ep85B and Ep85B-KLH immunized mice on days 0 and 49 exhibited 1.9 and 2.2 fold increases in Ep85B-IgM antibody responses, respectively. After the fourth and final dose, 50% of Ep85B immunized mice and 60% of Ep85B-KLH immunized mice were seroconverted. No Ep85B IgA antibody response was detected in either cohort.

Cross reactivity of Ep85B IgG antibody with Ag85B whole antigen

To determine whether anti Ep85B-IgG antibodies recognize the entire Ag85B antigen, immune responses were measured using sera from mice immunized with either Ep85B or Ep85B-KLH (Fig. 5). Significant increases in anti-Ag85B IgG responses were detected, and these were comparable to anti-Ep85B IgG responses in terms of both magnitude as well as responder frequency. No significant levels of anti-BSA IgG responses were detected in mice immunized with either Ep85B or Ep85B-KLH, thus indicating that immunization with Ep85B generates specific antibody responses which are capable of binding to the whole Ag85B antigen.

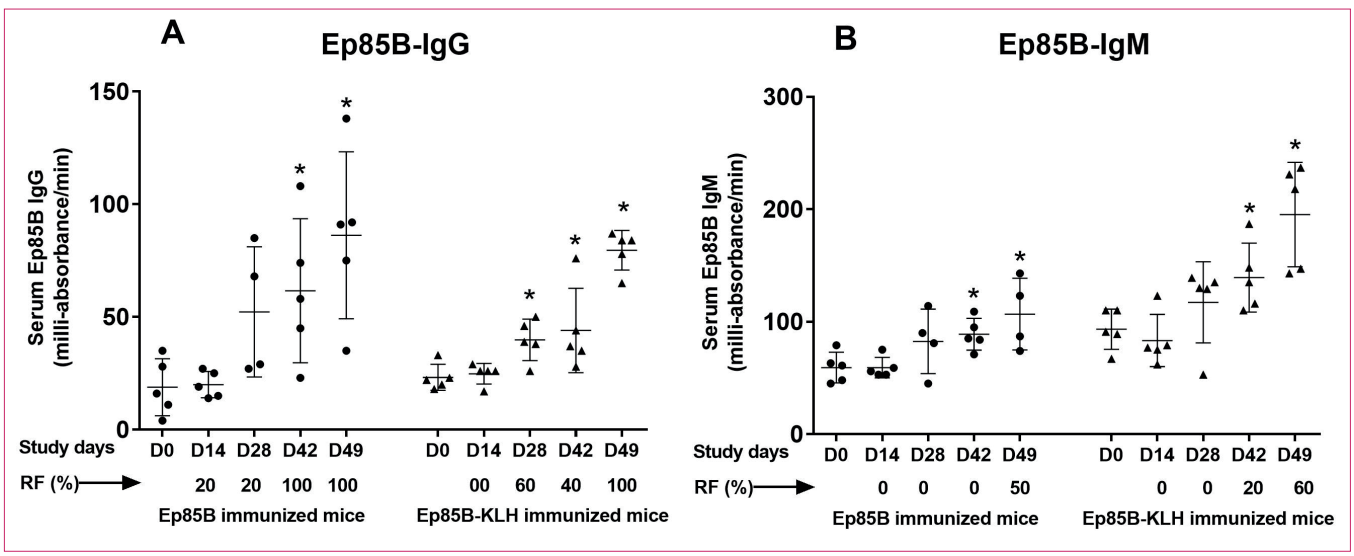

Figure 4. a, b. Ep85B IgG (a) and IgM (b) antibody responses in mice immunized with Ep85Bor Ep85B-KLH. The circular and triangular dark-filled dots indicate IgG and IgM responses of individual mouse immunized with Ep85B and Ep85B-KLH respectively. Study days and responder frequencies (RF) are listed. An asterisk denotes a statistically significant difference ($p<0.05$) compared to the baseline (day 0) performed by unpaired parametric t-test. The error bars represent standard errors of the mean. Data are shown from one immunization experiment, n=4–6.

Turk J Immunol 2018; 6(3):108–117

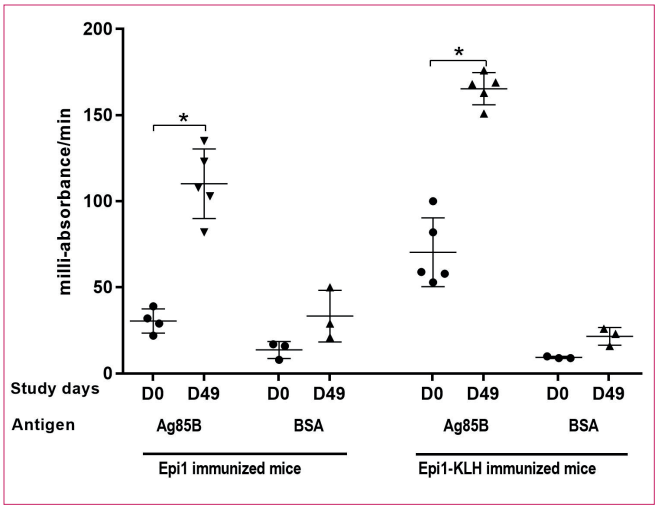

Figure 5. Cross reactivity of Ep85B IgG antibody to Ag85B antigen. The circular and triangular dark-filled dots indicate IgG responses to Ag85B of individual mouse immunized with Ep85B or Ep85B-KLH on day 0 and 49 respectively. The responder frequency is also listed. An asterisk denotes a statistically significant difference ($p<0.05$) compared to the baseline (day 0) performed by unpaired parametric t-test. The error bars represent standard errors of the mean. Data are shown from one immunization experiment, n=4-5.

Discussion

We have previously identified an immunogenic mycobacterial peptide composed of a 28 amino acid multi-epitope cluster with the potential to elicit T-cell responses *in vitro* in human whole blood cells.[25] In this study, we have employed a similar immuno-informatics pipeline to determine the suitability of this region, designated Ep85B, for immunizations in mice, since experimentally defined murine epitopes previously reported overlap only partially with our sequence.[36] In accordance with our *in silico* findings, we have demonstrated that this region harbors the potential to elicit both cell-mediated and humoral immune responses *in vivo*-findings that are consistent with the rationale behind a peptide-based vaccine design approach.

Although a plethora of bioinformatics approaches have been used to design vaccine candidates against various diseases[37–40], including TB[41], their immunogenic potentials have rarely been validated in laboratory experiments. In this study, we utilized a range of different algorithms to assess the suitability of Ep85B for *in vivo* immunizations using BALB/c mice. Protective immunity to TB is conferred by type 1 Th (Th1) cells, and several groups have shown that an effective vaccine requires the generation of a T cell-mediated immune response.[14,18,42,43] Relative to the comprehensiveness of its human HLA database, however, the IEDB platform features only a partial subset of all available murine MHC molecules. This limiting factor may account for the very low unique allele counts observed in our T cell epitope predictions.

Immunologic resistance to intracellular pathogens is mediated by specific patterns of cytokine secretion. In mice that are resistant to TB, protective immunity to mycobacterial infection is associated with high levels of IFN-γ, IL-2 and TNF-α (a Th1 cellular immune response), whereas lymphocyte production of IL-4 and overall Th2-like activity is dominant in susceptible strains.[44–47] In the same manner, it has been reported that susceptible BALB/c mice activate the Th2 compartment during both BCG vaccination as well as stimulation with Ag85, while resistant C57BL/6 mice mount a strong Th1 immune response.[48] However, studies have shown that a combined Th1/Th2 profile offers more efficacious protection than one preferentially skewed towards Th1 cells[49], and as such it is possible that the mixed responses we observed may be capable of conferring protection. Although the possibility of presentation of the peptide through MHC class-I and activation of cytotoxic T lymphocytes (CTL) cannot be completely ruled out, cytokine responses in in vitro assay using splenocytes from the mice immunized with Ep85B mostly indicated the activation of Th cells upon interaction with the peptide presented through MHC class-II. However, as a direct evidence of activation of Th cells by the algorithm-predicted epitopes, MHC tetramer assay could be done in future.

In addition to cellular immunity, antibody-mediated responses may play a significant role in protection against TB, and mycobacterial-specific monoclonal antibodies have been shown to elicit protective immune responses in mice.[50,51] We predicted the presence of probable antibody binding positions within Ag85B to detect any overlaps between putative B cell epitopes and the 28 aa T cell epitope cluster. The Kolaskar Tangaokar and ABCpred algorithms indicated the presence of a number of linear epitopes in Ag85B. However, B cell identification is complicated and need to consider the conformational aspects of the antigen and structure-function relationships of neutralizing antibodies.[1,52] Accordingly, the level of *in vivo* antibody production observed in our experiments was lower than expected when compared to the *in silico* binding predictions. A discontinuous epitope comprising residues situated on different positions of the full-length Ag85B peptide, designed on the basis of structure rather than only function, may be more suitable for eliciting humoral immune responses.[53]

We supplemented one animal cohort by delivering Ep85B in conjugation with the carrier protein KLH, as it has been widely used for delivering small peptide vaccines.[54–56] While both Ep85B and Ep85B-KLH immunized mice produced significant amounts of antibodies, no statistical difference was observed between cytokine profiles elicited by each of the two immunized animal cohorts. This suggests that the Ep85B cluster is capable of stimulating cell-mediated immune responses without conjugation to a carrier protein. However, the optimal efficacy elicited by a vaccine candidate frequently depends on the nature of the adjuvant or immunostimulant used, particularly for peptide vaccines which have simplified, defined structures.[44] Certain vaccines, including Ag85B-based fusion proteins, induce potent cellular immune responses when delivered in Th1 adjuvants[57,58], whereas others that generate consistent Th1-biased cell immunity grant less effective protection compared to adjuvants that elicit a mixed response.[49] Unlike the direct stimulation of lymphocytes by antigenic epitopes, adjuvants enhance the cell-mediated and humoral immune responses through the triggering of the activation of innate immune system e.g. facilitation of MHC-I antigen presentation pathway, activation of dendritic cells and induction of type-I interferon production.[59–62] As a result, no antigen specific T or B-cell responses are expected from immunization of mice with only adjuvant in the absence of epitope.[59] Therefore, no cohort was immunized with only adjuvant. However, the possibility of contribution/involvement of mycobacterial components in Complete Freund's Adjuvant in the overall immune response cannot be ruled out. Apart from Incomplete Freund's Adjuvant, dimethyl dioctadecyl ammoniumbromide (DDA), RIBI adjuvant, Quil-A saponin, and aluminum hydroxide could be potential adjuvant alternatives.[63] The dose of the antigen or adjuvant is also of importance, with minute changes in concentration may result in significantly reduced numbers of poly-functional T cells.[64] Further studies involving dosage modulation or the administration of booster doses may lead to more robust and appropriate patterns of immune responses. When an antigen is internalized and chopped inside an antigen presenting cell, it is divided into many epitopes. Among them only a few epitopes serve as immune-dominant epitope and generate strong immune response. The other epitopes may function as immunosuppressive epitopes, bind with immune cells and suppress the immune responses. Therefore, those immunosuppressive epitopes may lower the overall immune responses elicited by the antigen.[65] In this current study, we selected only the immune-dominant epitopes using immuno-informatics approaches, thereby we believe multi-epitope peptide will generate strong immune response. comparative immune responses between the groups of mice immunized with multi-epitope peptide or the whole Ag85B antigen are yet to be elucidated. It would also be important to investigate how efficient the epitope is to elicit immune responses in humans. It could be done by using humanized mice model offering functional human immune system in mice.[66]

Peptide vaccines, particularly those engineered through bioinformatics-aided design, can reliably overcome several burdens imposed by traditional vaccination strategies. Our *in vivo* observations using the Ep85B multi-epitope cluster, originally predicted and subsequently verified by a host of immuno-informatics tools, further validate the possibility of using computational approaches for the identification of antigenic determinants in other proteins of interest, thus promoting a greater understanding of strategies necessary for next-generation vaccine design and development.

Conclusions

Immunization of mice with Ep85B, an epitope within the mycobaterial protein Ag85B, can induce both cell-mediated and humoral responses. This study provides the evidence for the utility of an *in silico* predictive strategy in developing the next generation epitope vaccines.

Supplementary Materials: The following are available online at www.mdpi.com/link, Table 1. Th cell epitopes in Ep85B and their restricted murine MHC Class II molecules as predicted by the NN-align, ARBpython and SMM-align methods. Table 2. CTL cell epitopes in Ep85B and their restricted murine MHC Class I molecules as predicted by the ANN, ARB and SMM methods.

Acknowledgments: This research study was funded by ICDDR,B's core donors and Grand Challenges Explorations initiative Bill & Melinda Gates Foundation (BMGF), grant number OPP1058489. ICDDR,B acknowledges with gratitude the commitment of BMGF to its research efforts. ICDDR,B also gratefully acknowledges the following donors who provide unrestricted support: Government of the People's Republic of Bangladesh; the Department of Foreign Affairs, Trade and Development (DFATD), Canada; Swedish International Development Cooperation Agency (Sida) and the Department for International Development, (UKAid).

Ethics Committee Approval: Approved by the Research Review Committee (RRC) and Animal Experiments Ethics Committee (AEEC) of the International Centre for Diarrhoeal Disease Research, Bangladesh (ICDDR,B).

Peer-review: Externally peer-reviewed.

Author Contributions: S.M.T.I., S.Z., T.R.B., F.Q., and Z.I.S. conceived idea, designed experiments and prepared manuscript. S.M.T.I, S.Z., M.K.K., M.I.U., S.C., N.S.N., N.I., and M.M.A. performed experiments, applied algorithms and analyzed data.

Conflicts of Interest: None of the authors has any conflict of interest associated with this study. The funders had no role in study design, data collection and analysis, decision to publish, or preparation of the manuscript.

References

1. Korber B, LaBute M, Yusim K. Immunoinformatics comes of age. PLoS Comput Biol 2006;2:e71. [CrossRef]
2. De Groot AS, Bosma A, Chinai N, Frost J, Jesdale BM, Gonzalez

MA, et al. From genome to vaccine: in silico predictions, ex vivo verification. Vaccine 2001;19:4385–95. [CrossRef]

3. Maher D, Dye C, Floyd K, Pantoja A, Lonnroth K, Reid A, et al. Planning to improve global health: the next decade of tuberculosis control. Bull World Health Organ 2007;85:341–7. [CrossRef]
4. Zumla A, George A, Sharma V, Herbert N, Ilton BM. WHO's 2013 global report on tuberculosis: successes, threats, and opportunities. Lancet 2013;382:1765–7. [CrossRef]
5. Mustafa AS. Development of new vaccines and diagnostic reagents against tuberculosis. Mol Immunol 2002;39:113–9. [CrossRef]
6. Pym AS, Brodin P, Majlessi L, Brosch R, Demangel C, Williams A, et al. Recombinant BCG exporting ESAT-6 confers enhanced protection against tuberculosis. Nat Med 2003;9:533–9. [CrossRef]
7. Kagina BMN, Abel B, Scriba TJ, Hughes EJ, Keyser A, Soares A, et al. Specific T cell frequency and cytokine expression profile do not correlate with protection against tuberculosis after bacillus Calmette-Guerin vaccination of newborns. Am J Respir Crit Care Med 2010;182:1073–9. [CrossRef]
8. Martin C. The dream of a vaccine against tuberculosis; new vaccines improving or replacing BCG? Eur Respir J 2005;26:162–7. [CrossRef]
9. Aagaard C, Dietrich J, Doherty M, Andersen P. TB vaccines: current status and future perspectives. Immunol Cell Biol 2009;87:279–86. [CrossRef]
10. Kaufmann SH. Tuberculosis vaccine development: strength lies in tenacity. Trends Immunol 2012;33:373–9. [CrossRef]
11. Kaufmann SH. Fact and fiction in tuberculosis vaccine research:10 years later. Lancet Infect Dis 2011;11:633–40. [CrossRef]
12. Seder RA, Darrah PA, Roederer M. T-cell quality in memory and protection: implications for vaccine design. Nat Rev Immunol 2008;8:247–58. [CrossRef]
13. Hoft DF. Tuberculosis vaccine development: goals, immunological design, and evaluation. Lancet 2008;372:164–75. [CrossRef]
14. Flynn JL, Chan J, Triebold KJ, Dalton DK, Stewart TA, Bloom BR. An essential role for interferon gamma in resistance to Mycobacterium tuberculosis infection. J Exp Med 1993;178:2249–54. [CrossRef]
15. Derrick SC, Yabe IM, Yang A, Morris SL. Vaccine-induced anti-tuberculosis protective immunity in mice correlates with the magnitude and quality of multifunctional CD4 T cells. Vaccine 2011;29:2902–9. [CrossRef]
16. Cooper AM, Khader SA. The role of cytokines in the initiation, expansion, and control of cellular immunity to tuberculosis. Immunol Rev 2008;226:191–204. [CrossRef]
17. Flynn JL, Goldstein MM, Chan J, Triebold KJ, Pfeffer K, Lowenstein CJ, et al. Tumor necrosis factor-alpha is required in the protective immune response against Mycobacterium tuberculosis in mice. Immunity 1995;2:561–72. [CrossRef]
18. Cooper AM, Dalton DK, Stewart TA, Griffin JP, Russell DG, Orme IM. Disseminated tuberculosis in interferon gamma gene-disrupted mice. J Exp Med 1993;178:2243–7. [CrossRef]
19. Wang TT, Tan GS, Hai R, Pica N, Ngai L, Ekiert DC, et al. Vaccination with a synthetic peptide from the influenza virus hemagglutinin provides protection against distinct viral subtypes. Proc Natl Acad Sci U S A 2010;107:18979–84. [CrossRef]
20. Othoro C, Johnston D, Lee R, Soverow J, Bystryn JC, Nardin E. Enhanced immunogenicity of Plasmodium falciparum peptide vaccines using a topical adjuvant containing a potent synthetic Toll-like receptor 7 agonist, imiquimod. Infect Immun 2009;77:739–48. [CrossRef]
21. Liang B, Zhang Z, Inserra P, Jiang S, Lee J, Garza A, et al. Injection of T-cell receptor peptide reduces immunosenescence in aged C57BL/6 mice. Immunology 1998;93:462–8. [CrossRef]
22. Rosenberg SA, Yang JC, Schwartzentruber DJ, Hwu P, Marincola FM, Topalian SL, et al. Immunologic and therapeutic evaluation of a synthetic peptide vaccine for the treatment of patients with metastatic melanoma. Nat Med 1998;4:321–7. [CrossRef]
23. Phanuphak P, Teeratakulpixarn S, Sarangbin S, Nookhai S, Ubolyam S, Sirivichayakul S, et al. International clinical trials of HIV vaccines: I. Phase I trial of an HIV-1 synthetic peptide vaccine in Bangkok, Thailand. Asian Pac J Allergy Immunol 1997;15:41–8.
24. Francis JN, Bunce CJ, Horlock C, Watson JM, Warrington SJ, Georges B, Brown CB. A novel peptide-based pan-influenza A vaccine: A double blind, randomised clinical trial of immunogenicity and safety. Vaccine 2015:33:396–402. [CrossRef]
25. Khan MK, Zaman S, Chakraborty S, Chakravorty R, Alam MM, Bhuiyan TR, et al. In silico predicted mycobacterial epitope elicits in vitro T-cell responses. Mol Immunol 2014;61:16–22. [CrossRef]
26. Nielsen M, Lundegaard C, Worning P, Lauemøller SL, Lamberth K, Buus S, et al. Reliable prediction of T-cell epitopes using neural networks with novel sequence representations. Protein Sci 2003;12:1007–17. [CrossRef]
27. Bui HH, Sidney J, Peters B, Sathiamurthy M, Sinichi A, Purton KA, et al. Automated generation and evaluation of specific MHC binding predictive tools: ARB matrix applications. Immunogenetics 2005;57:304–14. [CrossRef]
28. Peters B, Sette A. Generating quantitative models describing the sequence specificity of biological processes with the stabilized matrix method. BMC Bioinformatics 2005;6:132. [CrossRef]
29. Nielsen M, Lund O. NN-align. An artificial neural network-based alignment algorithm for MHC class II peptide binding prediction. BMC Bioinformatics 2009;10:296. [CrossRef]
30. Nielsen M, Lundegaard C, Lund O. Prediction of MHC class II binding affinity using SMM-align, a novel stabilization matrix alignment method. BMC Bioinformatics 2007;8:238. [CrossRef]
31. Lundegaard C, Lamberth K, Harndahl M, Søren Buus, Lund O, Nielsen M. NetMHC-3.0: accurate web accessible predictions of human, mouse and monkey MHC class I affinities for peptides of length 8–11. Nucleic Acids Res 2008;36:W509–12. [CrossRef]
32. Sercarz EE, Maverakis E. Mhc-guided processing: binding of large antigen fragments. Nat Rev Immunol 2003;3:621–9. [CrossRef]
33. Kolaskar AS, Tongaonkar PC. A semi-empirical method for prediction of antigenic determinants on protein antigens. FEBS Lett 1990;276:172–4. [CrossRef]
34. Saha S, Raghava GP. Prediction of continuous B-cell epitopes in an antigen using recurrent neural network. Proteins 2006;65:40–8. [CrossRef]
35. Hartigan JA. Clustering Algorithms. USA: John Wiley & Sons, Inc; 1975. 351 p.

36. D'Souza S, Rosseels V, Romano M, Tanghe A, Denis O, Jurion F, et al. Mapping of murine Th1 helper T-Cell epitopes of mycolyl transferases Ag85A, Ag85B, and Ag85C from Mycobacterium tuberculosis. Infect Immun 2003;71:483–93. [CrossRef]
37. Chakraborty S, Chakravorty R, Ahmed M, Rahman A, Waise TM, Hassan F, et al. A computational approach for identification of epitopes in dengue virus envelope protein: a step towards designing a universal dengue vaccine targeting endemic regions. In Silico Biol 2010;10:235–46. [CrossRef]
38. Lopez JA, Weilenman C, Régine A, Roggero MA, Bonelo A, Tiercy JM, et al. A synthetic malaria vaccine elicits a potent CD8(+) and CD4(+) T lymphocyte immune response in humans. Implications for vaccination strategies. Eur J Immunol 2001;31:1989–98. [CrossRef]
39. Knutson KL, Schiffman K, Disis ML. Immunization with a HER-2/neu helper peptide vaccine generates HER-2/neu CD8 T-cell immunity in cancer patients. J Clin Invest 2001;107:477–84. [CrossRef]
40. Bourdette DN, Edmonds E, Smith C, Bowen JD, Guttmann CRG, Nagy ZP, et al. A highly immunogenic trivalent T cell receptor peptide vaccine for multiple sclerosis. Mult Scler 2005;11:552–61. [CrossRef]
41. Zvi A, Ariel N, Fulkerson J, Sadoff JC, Shafferman A. Whole genome identification of Mycobacterium tuberculosis vaccine candidates by comprehensive data mining and bioinformatic analyses. BMC Med Genomics 2008;1:18. [CrossRef]
42. Dalton DK, Pitts-Meek S, Keshav S, Figari I, Bradley A, Stewart T. Multiple defects of immune cell function in mice with disrupted interferon-gamma genes. Science 1993;259:1739–42. [CrossRef]
43. Orme IM, Roberts AD, Griffin JP, Abrams JS. Cytokine secretion by CD4 T lymphocytes acquired in response to Mycobacterium tuberculosis infection. J Immunol 1993;151:518–25.
44. Barnes PF, Lu S, Abrams JS, Wang E, Yamamura M, Modlin RL. Cytokine production at the site of disease in human tuberculosis. Infect Immun 1993;61:3482–9.
45. Zhang M, Lin Y, Iyer DV, Gong J, Abrams JS, Barnes PF. T-cell cytokine responses in human infection with Mycobacterium tuberculosis. Infect Immun 1995;63:3231–4.
46. Lowrie DB, Tascon RE, Bonato VL, Lima VM, Faccioli LH, Stavropoulos E, et al. Therapy of tuberculosis in mice by DNA vaccination. Nature 1999;400:269–71. [CrossRef]
47. Rook GA, Pando RH, Dheda K, Seah GT. IL-4 in tuberculosis: implications for vaccine design. Trends Immunol 2004;25:483–8. [CrossRef]
48. Huygen K, Abramowicz D, Vandenbussche P, Jacobs F, De Bruyn J, Kentos A, Drowart A, et al. Spleen cell cytokine secretion in Mycobacterium bovis BCG-infected mice. Infect Immun 1992;60:2880–6.
49. Fonseca DM, Silva CL, Paula MO, Soares EG, Marchal G, Horn C, Bonato VLD. Increased levels of interferon-gamma primed by culture filtrate proteins antigen and CpG-ODN immunization do not confer significant protection against Mycobacterium tuberculosis infection. Immunology 2007;121:508–17. [CrossRef]
50. Kozakiewicz L, Phuah J, JoFlynn A, Chan J. The role of B cells and humoral immunity in Mycobacterium tuberculosis infection. Adv Exp Med Biol 2013;783:225–50. [CrossRef]
51. Teitelbaum R, Freedman AG, Chen B, Robbins JB, Unanue E, Casadevall A, Bloom BR. A mAb recognizing a surface antigen of Mycobacterium tuberculosis enhances host survival. Proc Natl Acad Sci U S A 1998;95:15688–93. [CrossRef]
52. Blythe MJ, Flower DR. Benchmarking B cell epitope prediction: underperformance of existing methods. Protein Sci 2005;14:246–8. [CrossRef]
53. van Regenmortel MHV. Synthetic peptide vaccines and the search for neutralization B cell epitopes. The Open Vaccine Journal 2009;2:33–44. [CrossRef]
54. Fan J, Liang X, Horton MS, Perry HC, Citron MP, Heidecker GJ, et al. Preclinical study of influenza virus A M2 peptide conjugate vaccines in mice, ferrets, and rhesus monkeys. Vaccine 2004;22:2993–3003. [CrossRef]
55. Gilewski T, Adluri S, Ragupathi G, Zhang S, Yao TJ, Panageas K, et al. Vaccination of high-risk breast cancer patients with mucin-1 (MUC1) keyhole limpet hemocyanin conjugate plus QS-21. Clin Cancer Res 2000;6:1693–701.
56. Helling F, Shang A, Calves M, Zhang S, Ren S, Yu RK, et al. GD3 vaccines for melanoma: superior immunogenicity of keyhole limpet hemocyanin conjugate vaccines. Cancer Res 1994;54:197–203.
57. Dietrich J, Aagaard C, Leah R, Olsen AW, Stryhn A, Doherty TM, Andersen P. Exchanging ESAT6 with TB10 4 in an Ag85B fusion molecule-based tuberculosis subunit vaccine: efficient protection and ESAT6-based sensitive monitoring of vaccine efficacy. J Immunol 2005;174:6332–9. [CrossRef]
58. Agger EM, Rosenkrands I, Olsen AW, Hatch G, Williams A, Kritsch C, et al. Protective immunity to tuberculosis with Ag85B-ESAT-6 in a synthetic cationic adjuvant system IC31. Vaccine 2006;24:5452–60. [CrossRef]
59. Coffman RL, Sher A, Seder RA. Vaccine adjuvants: putting innate immunity to work. Immunity 2010;33:492–503. [CrossRef]
60. McCartney S, Vermi W, Gilfillan S, Cella M, Murphy TL, Schreiber RD, et al. Distinct and complementary functions of MDA5 and TLR3 in poly (I. C)-mediated activation of mouse NK cells. J Exp Med 2009;206:2967–76. [CrossRef]
61. McKee AS, Munks MW, Marrack P. How do adjuvants work? Important considerations for new generation adjuvants. Immunity 2007;27:687–90. [CrossRef]
62. O'Hagan DT, De Gregorio E. The path to a successful vaccine adjuvant –'the long and winding road'. Drug Discov Today 2009;14:541–51. [CrossRef]
63. Lindblad EB, Elhay MJ, Silva R, Appelberg R, Andersen P. Adjuvant modulation of immune responses to tuberculosis subunit vaccines. Infect Immun 1997;65:623–9.
64. Aagaard C, Hoang TTKT, Izzo A, Billeskov R, Troudt J, Arnett K, et al. Protection and polyfunctional T cells induced by Ag85B-TB10 4/IC31 against Mycobacterium tuberculosis is highly dependent on the antigen dose. PLoS One 2009;4:e5930. [CrossRef]
65. Mitchison N. Specialization, tolerance, memory, competition, latency, and strife among T cells. Annu Rev Immunol 1992;10:1–12. [CrossRef]
66. Akkina R. Humanized Mice for Studying Human Immune Responses and Generating Human Monoclonal Antibodies. Microbiol Spectr 2014;2. [CrossRef]